pVT Measurements and Related Studies on the Binary System $nC_{16}H_{34}$ - $nC_{17}H_{36}$ and on $nC_{18}H_{38}$ at High Pressures

Albert Würflinger, Denise Mondieig[a], Fazil Rajabalee[a], and Miquel Angel Cuevas-Diarte[b]

Institute of Physical Chemistry II, Ruhr University, D-44780 Bochum, Germany
[a] Centre de Physique Moléculaire Optique et Hertzienne, UMR 5798 au CNRS, Université Bordeaux I, 351 Cours de la Libération, F-33405 Talence Cedex, France
[b] Departament de Cristallografia, Mineralogia i Dipòsits Minerals, Facultat de Geologia, Universitat de Barcelona, c/Marti i Franquès, E-08028 Barcelona, Spain

Reprint requests to Prof. Dr. A. W.; Fax: +49-234-32-14183;
E-mail: Albert.Wuerflinger@ruhr-uni-bochum.de

Z. Naturforsch. **56 a,** 626–634 (2001); received July 18, 2001

The phase diagram of the binary system $nC_{16}H_{34}$ - $nC_{17}H_{36}$ has been established at ambient pressure using DSC and crystallographic measurements. At low temperatures below the rotator phase RI there exist two crystal forms Op (about $x(C_{17}) = 0.25$) and Mdci (about $x(C_{17}) = 0.67$) which are different from the crystal structures of the pure compounds (Tp for C_{16} and Oi for C_{17}). Furthermore two compositions: (a) $C_{16}/C_{17} = 3{:}1$ and (b) = 1:2, which correspond to the coexistence range of Op and Mdci, were chosen for high pressure DTA and *pVT* measurements, yielding the following findings: The specific volume of the rotator phase of C_{17} is distinctly lower than those of the binary systems at the same state point. Assuming the existence of a metastable rotator phase for C_{16}, an excess volume of $\Delta V^E/V \approx 0.01$ can be estimated. Due to the very enlarged coexistence range of RI, the mixtures reach their lower transition point at considerably lower temperatures (in isobaric measurements) or higher pressures (in isothermal measurements), where the specific volume is lower than that of C_{17} at its transition point. Furthermore, the volume and enthalpy changes of the Φ_{ord} – RI transition is distinctly smaller for the binary systems than for pure C_{17}. Thus the specific volumes of the phases Op and Mdci are appreciably larger than v(spec.) of C_{17}. Op and Mdci have practically the same specific volume in accordance with the crystallographic results. Enthalpy values are obtained with the aid of the Clausius-Clapeyron equation which agree well with enthalpies derived from the DSC measurements.

Furthermore, *pVT* data have been established for the liquid and solid phases of $nC_{18}H_{38}$ in the neighbourhood of the melting curve, allowing to determine volume and enthalpy changes of melting as a function of pressure.

Key words: Hexadecane, Heptadecane, Octadecane, *pVT*, Excess Volume, Phase Transition, High Pressure, X-ray.

1. Introduction

The thermodynamic properties of *n*-alkanes C_nH_{2n+2} (abbreviated by C_n) play an important role for energy storage applications; especially multi-component systems are used as thermal protection materials [1 - 4]. Many binary and ternary systems have been systematically investigated in the past [5 - 10], in particular the thermal and crystallographic properties of the solid rotator and low-temperature ordered phases have been studied. However, volumetric properties for solid mixed phases are only scarcely reported in literature. In a previous high-pressure DTA study on the system C_{19}/C_{21} some volumetric features were discussed [11]. However the volume data were derived from transition enthalpies with the aid of the Clausius-Clapeyron equation. In the present work we present directly measured volume data for the binary system C_{16}/C_{17}. The phase diagram of the system C_{16}/C_{17} was recently established at ambient pressure by Rajabalee [12]. At low temperatures below the rotator phase RI there are two crystal forms (Φ_{ord}) Op (about $x(C_{17}) = 0.25$) and Mdci (about $x(C_{17}) = 0.67$) which are different from the crystal structures

0932–0784 / 01 / 0900–0626 $ 06.00

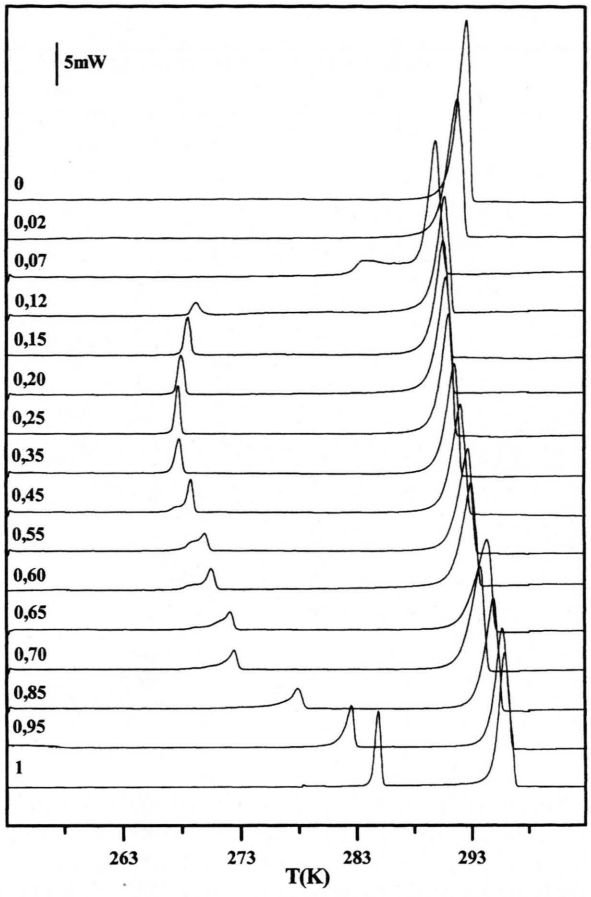

Fig. 1. Examples of DSC curves as a function of molar fraction in C_{17}.

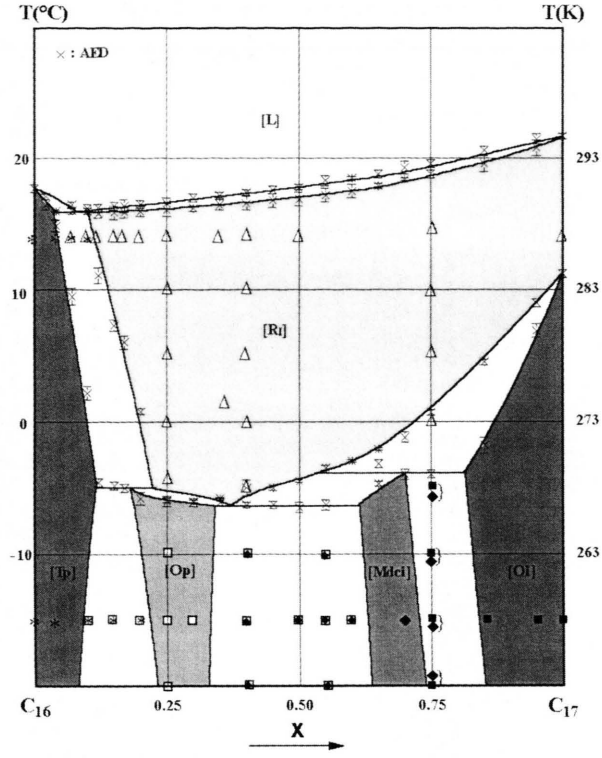

Fig. 2. Phase diagram of the binary system C_{16}/C_{17}.

of the pure compounds (Tp for C_{16} and Oi for C_{17}). Correspondingly, we have chosen two compositions for the high pressure studies: (a) C_{16}/C_{17} = 3:1 and (b) 1:2, which correspond to the coexistence range of Op and Mdci, respectively. The *pVT* data for the pure alkanes have been recently determined between 303 K and 343 K in steps of 10 K using an older pVT apparatus [13]. Changes in volume, enthalpy, and entropy along the phase transitions were reported. For the present study a new high pressure pVT apparatus [14, 15] is employed for the measurements on the two mixtures between 293 K and 313 K in steps of 5 K. Additionally measurements for C_{16} and C_{17} were retaken between 298 K and 313 K in steps of 5 K.

Octadecane is an interesting candidate, because its chain length is close to the series $n \geq 22$ of the even *n*-alkanes which exhibit a stable rotator phase [16]. For C_{20} a metastable rotator phase is observed on cooling [17]. For C_{18} a transient metastable rotator phase was reported [18]. C_{18} is also subject of a thorough molecular dynamics simulation [19].

2. Experimental Section

2.1. X-ray Powder Diffraction Measurements Analysis

Crystallographic measurements at selected temperatures were made using a Siemens D500 vertical powder diffractometer. A thin plate of glass was placed between the sample to be analysed and the sample holder in order to avoid the diffraction lines of copper and nickel, due to the holder, which disturb the analyses of the diffractograms. The data were collected with 0.05° 2θ-step and 3s-interval time. Diffraction measurements were also performed versus continuous temperature variations (inferior to $2K \cdot h^{-1}$) with a Guinier-Simon camera (GS). The copper Kα1 radiation (λ = 1.5406 Å) was used in both cases.

2.2. DSC Measurements

DSC measurements were carried out using a Perkin-Elmer DSC7 differential scanning calorimeter

Table 1. Transition temperatures (K) and enthalpies ($kJ \cdot mol^{-1}$) of mixed samples.

	— Melting —				— Transitions (Tp, Oi, Mdci, Op) → RI —			
$x(C_{17})$	T_{sol}	T_E	T_{liq}	ΔH	T_{solvi}	$T_{1,2,3}$	T_{solvs}	ΔH
0	290.7±0.3			53.0±1.6				
0.02	289.5±0.4		290.1±0.2	50.7±0.7				
0.04		289.0±0.1	289.7±0.4		287.9±0.5			
0.07		289.0±0.2	289.5±0.2		282.5±0.6			
0.10		289.0±0.2	289.2±0.3		275.2±0.5			
0.12	288.8±0.3		289.3±0.2	36.6±1.0		268.4±0.3	284.1±0.6	
0.13	289.0±0.2		289.4±0.1	36.6±0.8		268.5±0.2	284.0±0.5	
0.14	288.9±0.5		289.5±0.3	36.6±1.0		268.3±0.3	282.5±0.5	
0.15	288.9±0.4		289.4±0.3	36.6±1.0		268.2±0.3	280.3±0.4	
0.17	288.9±0.5		289.4±0.5	36.4±1.0		268.0±0.3	279.0±0.5	
0.20	289.0±0.4		289.6±0.3	36.5±1.0	267.2±0.5	—	273.8±0.2	
0.25	289.5±0.5		289.8±0.4	36.6±1.0	267.0±0.4		267.1±0.2	5.6±0.2
0.30	289.7±0.2		290.0±0.3	36.5±1.0	266.9±0.3		267.0±0.1	5.5±0.9
0.35	289.8±0.4		290.2±0.2	36.6±1.1	266.9±0.3		267.2±0.1	5.5±0.6
0.40	290.0±0.5		290.4±0.2	36.7±0.7		266.7±0.2	268.0±0.6	
0.45	290.2±0.5		290.6±0.3	36.8±1.0		266.7±0.3	268.0±0.2	
0.50	290.4±0.5		290.8±0.2	37.0±0.8		266.5±0.4	268.5±0.1	
0.55	290.7±0.5		291.3±0.4	37.3±0.9		266.7±0.4	269.5±0.2	
0.60	291.0±0.5		291.5±0.1	37.4±0.9		—	270.0±0.1	
0.65	291.3±0.2		291.8±0.3	37.6±1.0	268.3±0.2	269.8±0.3	270.9±0.1	
0.70	291.4±1.0		292.3±0.1	37.8±0.8	269.0±0.4		271.8±0.4	
0.75	291.8±0.3		292.6±0.3	38.1±1.0	269.0±0.3		273.7±0.2	
0.85	292.6±0.6		293.6±0.3	38.7±0.7	271.2±0.6		277.5±0.2	7.8±0.6
0.95	293.8±0.6		294.5±0.4	39.1±0.7	279.9±0.5		282.0±0.3	9.1±0.9
1	294.7±0.2			39.4±2.8	284.2±0.3			10.8±0.8

operating in the subambient mode. Transition temperatures and enthalpies were determined from four independent experiments on (4.0 ± 0.1) mg samples with $2 K \cdot min^{-1}$ speed of heating after temperature and energy calibration. Temperatures were determined from the DSC curves using the shape-factor method [20, 21]. The random part of the uncertainties was estimated using the Student's method with 95% threshold of reliability.

2.3. DTA Measurements under Pressure

DTA measurements were carried out with an equipment described previously [11, 22]. Samples of about 50 mg were enclosed in capsules made of indium. The soft metal serves to transmit the pressure (generated by compressed argon) without hysteresis. Thermograms are recorded both on heating and cooling. Transition temperatures are generally derived from the onset of the DTA peaks observed in heating runs at $2 K \cdot min^{-1}$.

2.4. pVT Measurements under Pressure

The new high-pressure apparatus [14, 15] allows repeated measurements with the same filling. Any volume change of the sample is transmitted to a piston, whose displacement is recorded inductively. Runs at increasing and decreasing pressure enable the determination of the hysteresis pressure. The corrected volume changes are combined with atmospheric pressure data in order to establish specific volumes in the whole *p,T* range. The densities at ambient pressure are either taken from literature or, if not available, are determined with a vibrating tube density meter Anton Paar.

2.5. Materials

For the DSC measurements the alkanes were obtained from Aldrich and Fluka with a purity better than 99.5%. For the high-pressure measurements the samples were purchased from Acros (purity 99%) and used without further purification.

3. Results and Discussion

3.1. Calorimetric Data and Phase Diagram of the Binary System

Seventeen binary mixed samples were studied combining DSC and X-ray diffraction measurements,

Table 2. Cell parameters or the analyzed phases.

x (C_{17})	a (Å)	b (Å)	c (Å)	T_f (K)	$T_f - 287$	V (Å^3)
Rotator phase RI (Fmmm, $z = 4$) at 287 K:						
0.15	7.76	5.06	45.34	289.4	2.4	1780
0.17	7.76	5.06	45.32	289.4	2.4	1780
0.20	7.78	5.06	45.46	289.5	2.5	1790
0.25	7.77	5.06	45.63	289.6	2.6	1794
0.35	7.75	5.05	45.80	290.2	3.2	1792
0.50	7.75	5.06	46.27	290.8	3.8	1814
0.75	7.71	5.07	46.79	292.6	5.6	1829
1	7.66	5.06	47.37	294.7	7.7	1836
Ordered phase Op ($Pca2_1$, $z = 4$) at 258 K:						
0.30	7.44	5.01	45.55			1698
Ordered phase Mdci (Aa, $\beta = 92.4°$, $z = 4$) at 258 K:						
0.70	7.43	5.01	46.59			1733

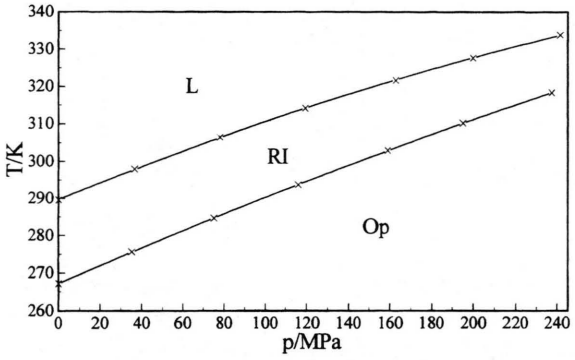

Fig. 3. $p(T)$ phase diagram of the binary sample C_{16}/C_{17} = 3 : 1.

typical DSC traces are shown in Figure 1. The phase diagram is presented in Fig. 2, showing one eutectic, two peritectoid and one eutectoid invariants. Below the freezing, the rotator phase RI is extended to a large range of temperatures and compositions. At low temperatures two new regions of mixed crystals are observed, Op for low concentration of C_{17} and Mdci for high concentration of C_{17}. The crystal form Tp exists only for $x(C_{16}) > 0.95$ and the Oi for $x(C_{17}) > 0.85$. Altogether there are 9 two-phase regions: [Tp+Op], [Op+Mdci], [Mdci+Oi], [RI+Oi], [RI+Mdci], [RI+Op], [RI+Tp], [Tp+L], [RI+L]. The transition temperatures for the solid - liquid equilibria (solidus: T_{sol}, liquidus: T_{liq}, and eutectic: T_E) and for the solid - solid equilibria (solvus superior, solvus inferior, peritectoid and eutectoid: $T_{1,2,3}$) together with the enthalpy changes derived from the DSC signals are entered in Table 1. For the mixtures, the melting enthalpy is clearly reduced compared with that

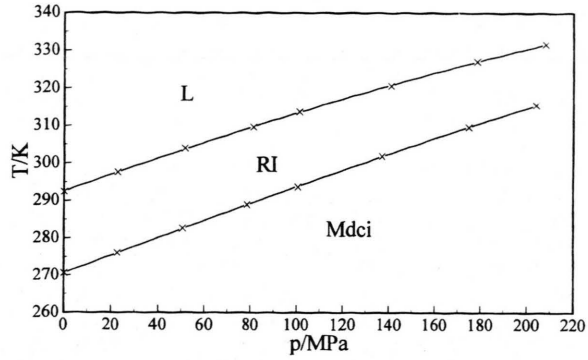

Fig. 4. $p(T)$ phase diagram of the binary sample C_{16}/C_{17} = 1 : 2.

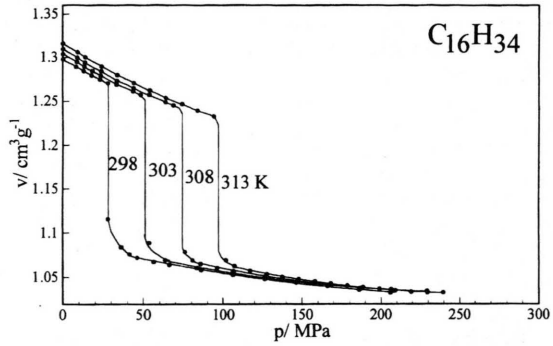

Fig. 5. Specific volumes of C_{16} as a function of pressure.

of the pure alkanes. Thus excess properties can be derived that have been thoroughly discussed for several homologues [6, 23]. For the rotational transition the enthalpy change is slightly lowered in comparison to C_{17}. This can be discussed in terms of excess properties as well, if a metastable rotator phase for n-C_{16} is accepted [12, 23, 24].

3.2. X-ray Diffraction

Details of the phase diagram presented above result from the X-ray diffraction patterns that allow to distinguish between the different crystal forms. At lower temperature the ordered phases were analysed at T = 258 K, the parameters for the rotator phase RI were determined at T = 287 K. The cell parameters of the analysed phases are presented in Table 2.

3.3. DTA Measurements under Pressure

The $p(T)$ phase diagrams for the mixed samples are displayed in Figs. 3 and 4. The transition from the

Table 3. Specific volumes ($cm^3 \cdot g^{-1}$) of $C_{16}H_{34}$ and $C_{17}H_{36}$.

	— *n*-hexadecane —				— *n*-heptadecane —			
p/	*T*/K:	*T*/K:	*T*/K:	*T*/K:	*T*/K:	*T*/K:	*T*/K:	*T*/K:
MPa	298.15	303.15	308.15	313.15	298.15	303.15	308.15	313.15
0.1	1.2982	1.3041	1.3100	1.3160	1.2906	1.2963	1.3020	1.3079
10	1.288	1.293	1.298	1.305	1.280	1.285	1.291	1.297
20	1.278	1.283	1.288	1.294	1.150	1.275	1.280	1.286
30	1.078	1.273	1.278	1.284	1.140	1.266	1.271	1.276
40	1.075	1.264	1.268	1.275	1.130	1.145	1.262	1.267
50	1.071	1.256	1.260	1.266	1.120	1.136	1.254	1.258
60	1.067	1.070	1.252	1.257	1.076	1.128	1.246	1.250
70	1.064	1.067	1.245	1.249	1.072	1.119	1.132	1.243
80	1.061	1.063	1.068	1.242	1.069	1.073	1.124	1.236
90	1.058	1.060	1.064	1.235	1.066	1.070	1.116	1.131
100	1.055	1.057	1.060	1.065	1.063	1.066	1.071	1.121
110	1.052	1.054	1.057	1.061	1.060	1.063	1.067	1.111
120	1.049	1.051	1.054	1.057	1.057	1.060	1.063	1.068
130	1.047	1.049	1.051	1.054	1.054	1.057	1.060	1.064
140	1.045	1.046	1.048	1.050	1.052	1.055	1.057	1.061
150	1.042	1.044	1.045	1.047	1.050	1.052	1.054	1.057
160	1.041	1.042	1.043	1.045	1.048	1.050	1.051	1.054
170	1.039	1.041	1.041	1.042	1.046	1.048	1.049	1.052
180	1.037	1.039	1.039	1.040	1.044	1.046	1.047	1.049
190	1.036	1.038	1.038	1.038	1.042	1.044	1.045	1.047
200	1.034	1.037	1.037	1.037	1.041	1.042	1.043	1.045

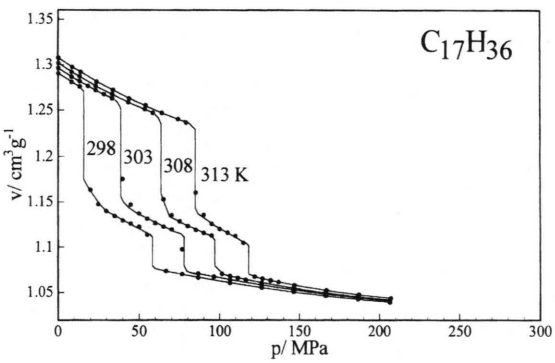

Fig. 6. Specific volumes of C_{17} as a function of pressure.

rotator to the low-temperature ordered phase is considerably shifted to lower temperatures in comparison to pure C_{17}. The curves converge slightly with increasing pressure, but there is no triple point in the pressure range studied as observed for pure C_{17}. The phase transition lines have been fitted to polynomials of second order and are entered (together with other thermodynamic properties to be discussed below) in Table 7.

3.4. pVT Measurements under Pressure

Pure C_{16} and C_{17}: The specific volumes for the pure alkanes are presented in Figs. 5 and 6, the steps

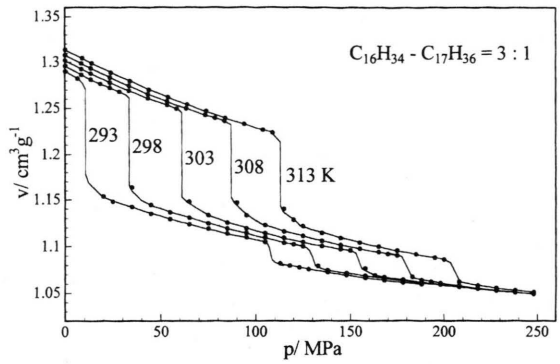

Fig. 7. Specific volumes for the C_{16} / C_{17} = 3 : 1 sample as a function of pressure.

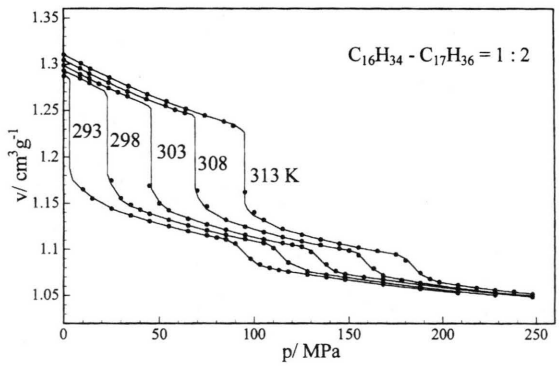

Fig. 8. Specific volumes for the C_{16} / C_{17} = 1 : 2 sample as a function of pressure.

indicating the volume change due to melting and transition to the rotator phase, respectively. For each isotherm and phase the $v(p)$-curves are fitted to polynomials which allow to calculate the specific volumes in steps of 10 MPa (Table 3). For 298 K and 303 K the agreement with previously reported data [13] is about 0.1%, for 313 K the deviation is ca. 0.3%. Different phases are separated in the Table by a horizontal line.

Binary samples: The specific volumes for the two binary samples are plotted as functions of pressure and temperatures between 293 and 313 K in Figs. 7 and 8, displaying the same sequences of steps as C_{17}. The pure alkanes fitted volume data are entered in the Tables 4 and 5. In Fig. 9 we compare the $v(p)$ behaviour with that of the pure alkanes at 303 K. Clearly, the phase region of the rotator phase has been enlarged for the mixtures in comparison to C_{17}, similarly to the observation at ordinary pressure, when the temperature is scanned.

Table 4. Specific volumes ($cm^3 \cdot g^{-1}$) of the binary system $C_{16}/C_{17} = 3 : 1$.

p/ MPa	T/K: 293.15	T/K: 298.15	T/K: 303.15	T/K: 308.15	T/K: 313.15
0.1	1.2904	1.2962	1.3021	1.3079	1.3139
10	1.278	1.285	1.291	1.297	1.303
20	1.153	1.275	1.281	1.287	1.293
30	1.145	1.267	1.272	1.277	1.283
40	1.139	1.147	1.264	1.268	1.274
50	1.132	1.140	1.256	1.260	1.265
60	1.126	1.134	1.249	1.252	1.257
70	1.121	1.128	1.136	1.245	1.249
80	1.116	1.122	1.129	1.239	1.242
90	1.111	1.116	1.123	1.132	1.235
100	1.107	1.111	1.117	1.126	1.229
110	1.083	1.107	1.111	1.119	1.223
120	1.079	1.102	1.106	1.114	1.124
130	1.075	1.098	1.102	1.108	1.118
140	1.072	1.074	1.099	1.104	1.112
150	1.068	1.071	1.095	1.099	1.107
160	1.066	1.068	1.070	1.095	1.102
170	1.063	1.065	1.067	1.092	1.097
180	1.061	1.063	1.064	1.089	1.093
190	1.059	1.060	1.061	1.064	1.090
200	1.057	1.058	1.059	1.060	1.086
210		1.056	1.056	1.057	1.061
220			1.054	1.055	1.058
230			1.052	1.053	1.055
240				1.051	1.053
250					1.051

Table 5. Specific volumes ($cm^3 \cdot g^{-1}$) of the binary system $C_{16}/C_{17} = 1 : 2$.

p/ MPa	T/K: 293.15	T/K: 298.15	T/K: 303.15	T/K: 308.15	T/K: 313.15
0.1	1.2873	1.2930	1.2988	1.3046	1.3105
10	1.155	1.283	1.288	1.294	1.300
20	1.148	1.273	1.277	1.283	1.289
30	1.140	1.150	1.268	1.274	1.280
40	1.134	1.142	1.260	1.265	1.271
50	1.128	1.135	1.146	1.257	1.262
60	1.122	1.129	1.138	1.250	1.255
70	1.117	1.123	1.130	1.143	1.247
80	1.113	1.118	1.124	1.135	1.241
90	1.109	1.113	1.118	1.128	1.235
100	1.082	1.109	1.113	1.122	1.131
110	1.079	1.105	1.108	1.116	1.125
120	1.075	1.078	1.105	1.111	1.119
130	1.072	1.075	1.101	1.106	1.113
140	1.069	1.072	1.076	1.102	1.108
150	1.066	1.069	1.072	1.099	1.104
160	1.064	1.066	1.069	1.096	1.100
170	1.061	1.063	1.067	1.070	1.096
180	1.059	1.061	1.064	1.067	1.093
190	1.057	1.058	1.061	1.063	1.067
200	1.054	1.056	1.059	1.060	1.064
210		1.054	1.056	1.057	1.061
220		1.052	1.054	1.055	1.058
230			1.052	1.053	1.055
240				1.051	1.053
250					1.052

From Fig. 9 one can derive the following conclusions: The specific volume of the rotator phase of C_{17} is distinctly lower than those of the binary systems *at the same state point* (e. g. 70 MPa, 303 K). However, due to the very enlarged coexistence range of RI the mixtures reach their lower transition point at considerably lower temperatures (in isobaric measurements) or higher pressures (in isothermal measurements), where the specific volume is lower than that of C_{17} at its transition point. Furthermore, the volume step to the low-temperature phase Φ_{ord} is distinctly smaller for the binary systems than for pure C_{17}. Thus the specific volumes of the phases Op and Mdci are appreciably larger than v(spec.) of C_{17}. Op and Mdci have practically the same specific volume in accordance with the crystallographic results. The volume change of melting is not so drastically changed, except that pure C_{16} (which does not possess a rotator phase) has of course the highest value.

It might be interesting to compare the densities at the transition points indicated (see Fig. 9) by a, b (melting) and c, d (rotational transition) for other temperatures. To this end we fit the $v(p)$ isotherms to

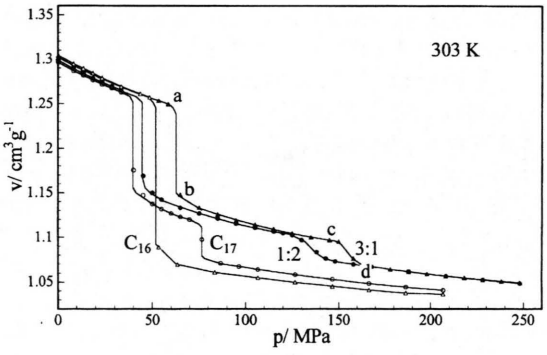

Fig. 9. Comparison of the specific volumes v for C_{16}, C_{17}, and the two binary samples at 303 K; a, b, c, d indicate the transition points.

polynomials, for each phase separately, and extrapolate them to the transition pressure. The results are plotted in Figure 10. The distance between a, b yields the volume change of melting, that of c, d the volume change of the rotational transition. The estimation of $\Delta V_{RI \rightarrow L}$ is particularly difficult because of the strong pre-transition behaviour. The curves a, b, c, d in turn

Table 6. Specific volumes along the phase transitions: $v/cm^3 \cdot mol^{-1} = A + B \cdot p/MPa$.

Trans.p.	Phase	C_{16}/C_{17} = 1:2		C_{16}/C_{17} = 3:1		C_{17}	
		A	$10^4 \cdot B$	A	$10^4 \cdot B$	A	$10^4 \cdot B$
a	L	1.2847	−5.778	1.2818	−5.379	1.2822	−5.835
b	RI	1.1632	−2.930	1.1617	−3.003	1.1578	−2.804
c	RI	1.1226	−1.669	1.1244	−1.955	1.1272	−1.868
d	Φ_{ord}	1.0987	−1.595	1.1047	−2.061	1.0848	−1.342

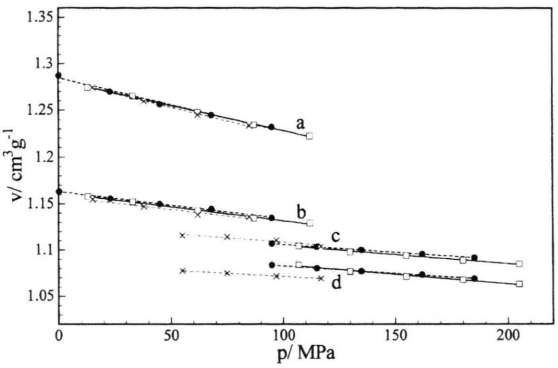

Fig. 10. Specific volumes at the phase transitions, ×: C_{17}, •: C_{16}/C_{17} = 1:2, □: C_{16}/C_{17} = 3:1.

have been fitted to straight lines and entered in Table 6. The constants A represent the specific volumes at atmospheric pressure. For the system C_{16}/C_{17} they are close to those derived from the crystallographic measurements: v = 1.108 $cm^3 \cdot g^{-1}$ for Op ($x(C_{17})$ = 0.3) and v = 1.104 $cm^3 \cdot g^{-1}$ for Mdci ($x(C_{17})$ = 0.7), compared with v = 1.105 $cm \cdot g^{-1}$ for C_{16}/C_{17} = 3:1 and v = 1.099 $cm^3 \cdot g^{-1}$ for C_{16}/C_{17} = 1:2. For the rotator phase we calculate from Table 2: v = 1.1745 $cm^3 \cdot g^{-1}$ for $x(C_{17})$ = 0.25 and v = 1.162 $cm^3 \cdot g^{-1}$ for $x(C_{17})$ = 0.75, compared with v = 1.1617 $cm \cdot g^{-1}$ for C_{16}/C_{17} = 3:1 and v = 1.632 $cm^3 \cdot g^{-1}$ for C_{16}/C_{17} = 1:2 at the point "b" below the freezing point. In the case of $C_{17}H_{36}$ the extrapolation is more favourable than in [13], because of the smaller temperature steps. Correspondingly v = 1.085 $cm^3 \cdot g^{-1}$ (1.089 [25]) and $\Delta V_{RI \rightarrow L}$ = 29.9 $cm^3 \cdot mol^{-1}$ (29.4 [26]) now agree better with literature (in parantheses). $\Delta H_{RI \rightarrow L}$ = 37.6 $kJ \cdot mol^{-1}$ is a bit lower than 39.4 $kJ \cdot mol^{-1}$ [17]. For the transition to the rotator phase one obtains: $\Delta V_{Cr \rightarrow RI}$ = 10.2 $cm^3 \cdot mol^{-1}$, $\Delta H_{Cr \rightarrow RI}$ = 11.1 $kJ \cdot mol^{-1}$ (10.8 $kJ \cdot mol^{-1}$) [17]. For C_{16} the following data are obtained: $\Delta V_{Cr \rightarrow L}$ = 45.3 $cm^3 \cdot mol^{-1}$ (45.7 [27]), $\Delta H_{Cr \rightarrow L}$ = 54.8 $kJ \cdot mol^{-1}$ (53.0 [17]), v_{Cr} = 1.083 $cm^3 \cdot g^{-1}$ (1.082 [25]), v_L = 1.2835 $cm^3 \cdot g^{-1}$. Enthalpy values are obtained with the aid of the Clausius-Clapeyron equation. The thermodynamic data for the binary systems are presented in Table 7. The necessary slopes dp/dT are derived from the fitted $T(p)$ curves, due to the DTA measurements, which are entered in Table 7 as well. Despite the insufficiencies of the enthalpy calculation the agreement with Rajabalee [12] is not too bad.

Table 7. Thermodynamic properties of the binary samples.

System	Transition	T/K	p/MPa	ΔV_m/($cm^3 \cdot mol^{-1}$)	ΔH_m/($kJ \cdot mol^{-1}$) Cl.-eq.[a]	Rajabalee [12]
C_{16}/C_{17} = 1:2	RI → L	$T(p)$/K = 292.47 + 0.22814 (p/MPa) − 1.91961·10^{-4} (p/MPa)^2				
		292.5	0.1	28.7	36.8	37.6
		303.4	100	22.0	30.2	
	Mdci → RI	$T(p)$/K = 270.52 + 0.24414 (p/MPa) − 1.16381·10^{-4} (p/MPa)^2				
		270.5	0.1	5.64	6.25	
		293.8	100	5.46	6.58	
		314.7	200	5.29	6.82	
C_{16}/C_{17} = 3:1	RI → L	$T(p)$/K = 289.76 + 0.22571 (p/MPa) − 1.79548·10^{-4} (p/MPa)^2				
		289.8	0.1	27.6	35.5	36.6
		310.5	100	22.2	30.5	
	Op → RI	$T(p)$/K = 267.17 + 0.24196 (p/MPa) − 1.10993·10^{-4} (p/MPa)^2				
		267.2	0.1	4.54	5.02	5.6
		290.2	100	4.79	5.75	
		311.1	200	5.03	6.48	

[a] from ΔV data using the Clausius-Clapeyron equation.

Excess volumes: Although C_{16} does not display a rotator phase, one can postulate the existence of a metastable one. Roblès has derived crystallographic data for several metastable phases by a suitable extrapolation from homologous n-alkanes of longer chain length [24]. The result for the metastable RI (Z = 4) of C_{16} is: a = 5.05 Å, b = 7.70 Å, c = 44.5 Å, yielding V = 1730 $Å^3$, and v(spec.) = 1.1505 $cm^3 \cdot g^{-1}$. The values of C_{17} are [24]: V = 1836 $Å^3$, and v(spec.) = 1.1494 $cm^3 \cdot g^{-1}$. Thus we obtain the excess volume of the rotator phase for the two studied samples: C_{16}/C_{17} = 3:1 : v^E = 0.012 $cm^3 \cdot g^{-1}$, C_{16}/C_{17} = 1:2 : v^E = 0.013 $cm^3 \cdot g^{-1}$. The positive v^E-value is clear, regarding the extra place which is needed to form a solid mixture of alkanes with different chain lengths. This has been discussed in literature since a long time [11].

At elevated pressures no data for a metastable rotator phase of C_{16} are available. However, regarding at 1 atm the close values of v(spec.) = 1.1505 $cm^3 \cdot g^{-1}$

Table 8. Excess volumes for the rotator phase of the binary samples studied.

	C_{16}/C_{17} = 1:2				C_{16}/C_{17} = 3:1		
p/	T/K:	T/K:	T/K:	T/K:	T/K:	T/K:	T/K:
MPa	298.15	303.15	308.15	313.15	298.15	303.15	308.15
30	0.0102						
40	0.0123				0.0170		
50	0.0149	0.0092			0.0198		
60		0.0101					
70		0.0116	0.0111			0.0177	
80			0.0112				
90			0.0120				0.0162
100				0.0106			
110				0.0139			

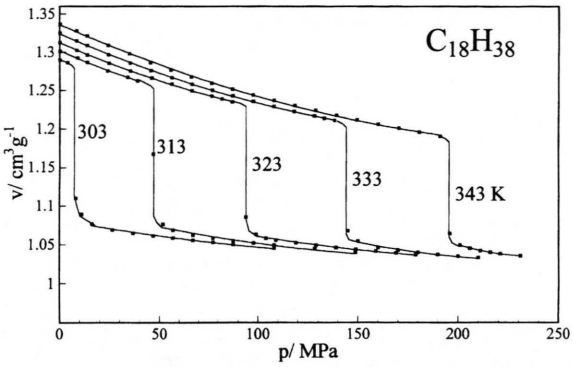

Fig. 11. Specific volumes of C_{18} as a function of pressure.

for C_{16} and 1.1494 $cm^3 \cdot g^{-1}$ for C_{17}, one may approximately consider the difference of v(mixt.) and $v(C_{17})$ using the Tables 3 - 5. The result is entered in Table 8, showing $v^E \approx 0.017$ $cm^3 \cdot g^{-1}$ for C_{16}/C_{17} = 3:1 and $v^E \approx 0.011$ $cm^3 \cdot g^{-1}$ for C_{16}/C_{17} = 1:2 with no significant pressure or temperature dependence. One has to take into consideration that the excess volumes can only be calculated in a small "$T(p)$ window" of overlapping rotator phases, that is close to "b" for the mixed samples (particularly for the sample 3:1) and close to "c" for pure C_{17} (cf. Fig. 9). Therefore the v^E-values seem to be systematically too high for the sample 3:1. For the sample 1:2 the results of Table 8 are in reasonable agreement with v^E derived from the atmospheric pressure data above.

For the low-temperature ordered phases one may estimate a positive excess volume as well, if hypothetical metastable phases Op and Mdci are assumed to exist for the pure compounds as well. However, an unambiguous extrapolation from the longer homologous members does not seem to be possible.

Table 9. Specific volumes ($cm^3 \cdot g^{-1}$) of C_{18}.

p/	T/K:	T/K:	T/K:	T/K:	T/K:
MPa	303.15	313.15	323.15	333.15	343.15
0.1	1.2900	1.3014	1.3130	1.3247	1.3367
10	1.077	1.291	1.301	1.313	1.325
20	1.073	1.280	1.291	1.302	1.314
30	1.069	1.271	1.281	1.292	1.304
40	1.065	1.262	1.272	1.282	1.294
50	1.061	1.073	1.263	1.273	1.284
60	1.058	1.068	1.255	1.264	1.275
70	1.055	1.064	1.247	1.256	1.266
80	1.052	1.059	1.240	1.248	1.258
90	1.049	1.055	1.234	1.241	1.250
100	1.047	1.052	1.061	1.234	1.242
110	1.045	1.048	1.057	1.227	1.235
120		1.045	1.053	1.221	1.228
130		1.043	1.050	1.216	1.222
140		1.040	1.046	1.211	1.216
150			1.043	1.053	1.211
160			1.041	1.048	1.206
170			1.039	1.044	1.201
180				1.040	1.197
190				1.037	1.193
200				1.035	1.050
210					1.043
220					1.039
230					1.036

Table 10. Thermodynamic properties of n-octadecane at the melting transition.

T/	p/	ΔV_m/	ΔH_m/	ΔS_m/
K	MPa	$cm^3 \cdot mol^{-1}$	$kJ \cdot mol^{-1}$	$J \cdot mol^{-1} \cdot K^{-1}$
301.26	0.1	52.43	63.43	210.5
303.15	7.9	51.51	63.14	208.3
313.15	50.4	46.79	61.31	195.8
323.16	95.7	42.40	58.84	182.1
333.16	144.3	38.43	55.59	166.9
343.15	197.1	34.96	51.39	149.8

Pure C_{18}: The specific volumes of octadecane is presented in Fig. 11, the fitted data are entered in Table 9. For liquid C_{18} other high pressure data are available for comparison [28, 29] which agree within 0.2%. Only for 343 K and pressures close to the melting the densities reported by Dutour et al. [28] are ca. 0.3% lower. The latter authors presented the atmospheric pressure densities (determined with an Anton Paar densimeter) by a smoothed polynomial function, which was also used in this work.

As for C_{16} and C_{17} we extrapolated the fitted v(spec.) isotherms to the melting pressure, yielding: $v_{liq}/cm^3g^{-1} = 1.2877 - 6.981 \cdot 10^{-4} + 1.0396 \cdot 10^{-6}$, $v_{cr}/cm^3g^{-1} = 1.0816 - 2.255 \cdot 10^{-4} + 4.10 \cdot 10^{-7}$, and

$\Delta V_{Cr \rightarrow L}/cm^3g^{-1} = 0.2061 - 4.726 \cdot 10^{-4} + 6.3 \cdot 10^{-7}$. Volume changes reported by Nelson et al. [30] are somewhat smaller. The atmospheric pressure value of v_{cr} (1.0816 cm^3g^{-1}) can be compared with crystallographic data. C_{18} crystallizes in the triclinic system that has been investigated by several authors: Craig et al. [25], V = 455.4 Å^3 ⇒ v(spec.) = 1.0778 cm^3g^{-1}; Roblès [24], T = 291 K, V = 463.3 Å^3 ⇒ v(spec.) = 1.0964 cm^3g^{-1}; Nyburg et al. [31], T = 295 K, V = 454.3 Å^3 ⇒ v(spec.) = 1.0753 cm^3g^{-1}.

The melting pressures (displayed as steps in Fig. 11) agree well with the melting line previously established by DTA [11]. The combined data set (from DTA and pVT measurements) is fitted to the polynomial: T/K = 301.2 + 0.2446 (p/MPa) – $1.619 \cdot 10^{-4}$(p/MPa)^2. Using the Clausius-Clapeyron equation, we calculated the melting enthalpy as a function of pressure, see Table 10. The atmospheric pressure value ΔH_m = 63.43 kJ·mol^{-1} is larger than 60.1 kJ·mol^{-1} reported by Roblès [24, 17], due to the somewhat too high volume change (0.206 cm^3g^{-1} compared with 0.1953 cm^3g^{-1} [30]) and the uncertainty of the initial slope dT/dp.

Acknowledgement

The collaboration was supported by "la Xarxa Temàtica Aliatges Moleculars de la Generalitat de Catalunya" and the "REALM" (Réseau Européen sur les Alliages Moléculaires). A.W. thanks the university of Bordeaux (France) for an invitation as "professeur invité" in march 2001.

[1] D. Mondieig, A. Marbeuf, L. Roblès, P. Espeau, P. Poirier, Y. Haget, T. Calvet-Pallas, and M. A. Cuevas-Diarte, High Temperatures – High Pressures **29**, 385 (1997).
[2] P. Espeau, D. Mondieig, Y. Haget, and M. A. Cuevas-Diarte, Packag. Technol. Sci. **10**, 253 (1997).
[3] M.A. Cuevas-Diarte, T. Calvet-Pallas, H. A. J. Oonk, D. Mondieig, and Y. Haget, Mundo scientifico **213**, 45 (2000).
[4] F. Arjona, T. Calvet-Pallas, M. A. Cuevas-Diarte, V. Métivaud, and D. Mondieig, Bol. Soc. Esp. Ceram. Vidrio **39**, 548 (2000).
[5] V. Métivaud, F. Rajabalee, D. Mondieig, Y. Haget, and M. A. Cuevas-Diarte, Chem. Mater. **11**, 117 (1999).
[6] F. Rajabalee, V. Métivaud, H.A.J. Oonk, D. Mondieig, and P. Waldner, Phys. Chem. Chem. Phys. **2**, 1345 (2000).
[7] F. Rajabalee, V. Métivaud, D. Mondieig, Y. Haget, and M. A. Cuevas-Diarte, Helv. Chim. Acta. **82**, 1916 (1999).
[8] V. Métivaud, F. Rajabalee, H. A. J. Oonk, D. Mondieig, Y. Haget, and M. A. Cuevas-Diarte, Can. J. Chem. **77**, 332 (1999).
[9] F. Rajabalee, V. Métivaud, D. Mondieig, Y. Haget, and H. A. J. Oonk, Chem. Mater. **11**, 2788 (1999).
[10] R. Stolk, F. Rajabalee, M. H. G. Jacobs, P. Espeau, D. Mondieig, H. A. J. Oonk, and Y. Haget, Calphad **21**, 401 (1998).
[11] A. Würflinger and G. M. Schneider, Ber. Bunsenges. Phys. Chem. **77**, 121 (1973).
[12] F. Rajabalee, European Label thesis, University of Bordeaux I, France, 1998.
[13] A. Würflinger and M. Sandmann, Z. Naturforsch. **55a**, 533 (2000).
[14] M. Sandmann, doctoral thesis, Ruhr-University of Bochum, Germany, 1998.
[15] A. Würflinger, M. Sandmann, and W. Weissflog, Z. Naturforsch. **55a**, 823 (2000).
[16] D. Mondieig, P. Espeau, L. Roblès, Y. Haget, H. A. J. Oonk, and M. A. Cuevas-Diarte, J. Chem. Soc. Faraday Trans. **93**, 3343 (1997).
[17] P. Espeau, L. Roblès, D. Mondieig, Y. Haget, M. A. Cuevas-Diarte, and H. A. J. Oonk, J. Chim. Phys. **93**, 1217 (1996).
[18] E. B. Sirota and A. B. Herhold: Scattering from Polymers, ACS Symposium Series **739** (P. Cebe, B. S. Hsiao, D. J. Lohse, eds.), Chapt. **15**, 232 (2000).
[19] A. Marbeuf et al., unpublished.
[20] R. Courchinoux, N. B. Chanh, Y. Haget, E. Tauler, and M. A. Cuevas-Diarte, Thermochimica Acta **128**, 45 (1988).
[21] R. Courchinoux, N. B. Chanh, Y. Haget, T. Calvet, E. Estop, and M. A. Cuevas-Diarte, J. Chim. Phys. **86**, 561 (1989).
[22] J. Reuter and A. Würflinger, Ber. Bunsenges. Phys. Chem. **99**, 1247 (1995).
[23] H.A.J. Oonk, D. Mondieig, Y. Haget, and M. A. Cuevas-Diarte, J. Chem. Phys. **108**, 715 (1998).
[24] L. Roblès, European Label thesis, University of Bordeaux I, France, 1995.
[25] S. R. Craig, G. P. Hastie, K. J. Roberts, and J. N. Sherwood, J. Mater. Chem. **4**, 977 (1994).
[26] A. Turturro and U. J. Bianchi, Chem. Phys. **62**, 1668 (1975).
[27] A. van Hook and L. Silver, J. Chem. Phys. **10**, 686 (1942).
[28] S. Dutour, J. L. Daridson, and B. Lagourette, Int. J. Thermophys. **21**, 173 (2000).
[29] W. G. Cutler, R. H. McMickle, W. Webb, and R. W. Schiessler, J. Chem. Phys. **29**, 727 (1958).
[30] R. R. Nelson, W. Webb, and J. A. Dixon, J. Chem. Phys. **33**, 1756 (1960).
[31] S. C. Nyburg and H. Luth, Acta Cryst. **B28**, 2992 (1972).